Springer

KSME

Journal of Mechanical Science and Technology 28 (12) (2014) 5143~5148
www.springerlink.com/content/1738-494x
DOI 10.1007/s12206-014-1138-7

Effect of process parameters on optimum welding condition of DP590 steel by friction stir welding †

Young Gon Kim*, Ji Sun Kim and In Ju Kim

Green Manufacturing Process R&D Group, Korea Institute of Industrial Technology, Gwangju, 500-460, Korea

(Manuscript Received April 10, 2014; Revised August 7, 2014; Accepted September 12, 2014)

Abstract

In the automotive industry, vehicle weight reduction techniques have been actively studied to improve the rate of fuel consumption and to cope with the regulation restricting exhaust gas. For this reason, advanced high-strength steel (AHSS) is preferred in the automobile industry as its tensile strength is 590 MPa and over. In this study, to obtain the optimum welding condition, the friction stir welding (FSW) process applied to AHSS was considered. The FSW experiment was performed on a stir plate using a Si_3N_4 tool and a 1.4-mm-thick DP590 steel sheet manufactured by cold rolling. In addition, to investigate the temperature distribution of the advancing and retreating sides in the welding state, the tool rotation speed of 800 rpm, and the welding speed of 180 mm/min, a K-type thermocouple was inserted in the backing plate, and the peak temperature was evaluated at each point. Especially, the correlation between the heat input per unit length and the formation of the FSW zone was minutely analyzed.

Keywords: Advanced high-strength steel; DP590; Heat input; Stir-in-plate

1. Introduction

The friction stir welding (FSW) process is one of the solid-state joining methods newly developed by The Welding Institute (TWI) in 1991 [1]. Frictional heat is generated between the wear-resistant welding tool and the workpiece. This heat, along with that generated by the mechanical mixing and within the material, cause the stirred materials to soften without melting. The FSW process practically prevents coarsening and welding deformation compared with an arc welding on behalf of fusion welding, and is an environment-friendly welding process that does not produce fumes and spatter, which are injurious to health [2-4]. For this reason, the application of the FSW process, which has many advantages, is growing in various fields, such as in the shipbuilding, automobile, railroad car, and civil structure industries [5-7].

In the automobile industry, the amount of 590 MPa-grade-and-over AHSS used is increasing due to the demand for fuel consumption and the exhaust gas regulation [8]. In spite of that, the research on AHSS involving the FSW process is virtually at a standstill due to the weak equipment available for use and the narrow applicability of the tool. To intensify the basic research on FSW, a practical study of the FSW process is urgently needed. The determination of the quality of the material and its geometry is most important according to the FSW principle. In many studies, tools made from SKD11 and SKD61, such as alloy steel tools for joining the typical non-ferrous alloys (Al and Mg alloys), were used [9-12], but it is difficult to find research results joining steel like high-melting-point metals through FSW. A major cause of this is that the low-priced tool is not satisfactory in terms of strength, wear resistance, and toughness at high temperatures compared with the expensive polycrystalline cubic boron nitride (PCBN) tool [13].

On the other hand, to ensure high welding quality on FSW joints, it is necessary to consider the appropriate approach for tool selection according to the material properties as well as the optimization of the welding parameters. The fundamental FSW parameters are the tool rotation speed; the traveling speed, which affects the heat input to the base metal and the tilting angle; and the plunge depth, which affects the metal flow. As mentioned earlier, the optimization of the welding parameters and the consideration of the heat input are important research tasks for widening the applicability of FSW.

Therefore, in this study, to apply FSW to high-strength steels such as high-melting-point metals, an experiment was carried out using a specially designed Si_3N_4 tool, after which a PCBN tool and a DP590 steel sheet were used for joining. To determine if the welding boundary satisfied the joint quality requirement, varied and combined welding parameters were used for the experiment. Besides, the relation between the heat input per unit length and the formation of FSW joints was

*Corresponding author. Tel.: +82 62 600 6290, Fax.: +82 62 600 6099
E-mail address: ygkim1@kitech.re.kr
† Recommended by Associate Editor Young Whan Park

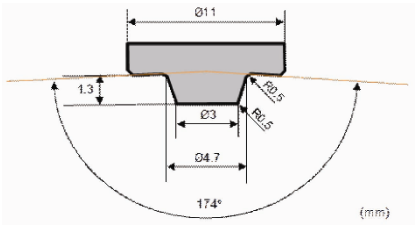

Fig. 1. FSW tool geometry.

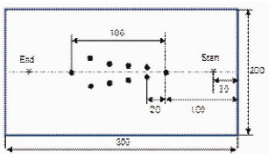

(a) Top view (work-piece)

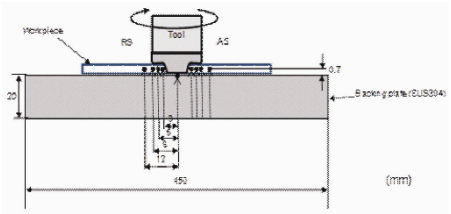

(b) Side view

Fig. 2. Peak temperature measurement points on the workpiece during FSW.

minutely analyzed to ensure the influence of the joint quality on the heat input.

2. Experimental procedures

Cold-rolled dual-phase (DP) steel plates 300 mm long, 100 mm wide, and 1.4 mm thick were used in this study. The major chemical composition of the base metal was 0.14C-1.5Mn-0.25Si-<0.025P-<0.01S (wt%). The microstructure had a distributed ferrite and martensite, and the tensile strength of the base metal was 590 MPa grade.

To evaluate the weldability for DP590, stir-in-plate was performed using a 2D FSW machine. The FSW tool was concave-type and was made up of Si_3N_4 material, as shown in Fig. 1. The peak temperature of the welded joint during FSW was measured using a K-type thermocouple, which was inserted in a plate through a small hole in the backing plate from the joint center, near the rotating probe, as shown in Fig. 2. The peak temperature was measured at four points: at the bottom side of the SZ (stirred zone), near the TMAZ (thermo-mechanically affected zone), at the HAZ (heat-affected zone), and at the base metal.

To investigate the optimum welding condition of DP590 FSW joints, major welding factors like rotation speed, traveling speed, and tilting angle were considered. Table 1 shows the process parameters for stir-in-plate. The variation of the tool insertion depth was also investigated.

Visual and X-ray radiography inspections were performed to reveal the joint defect at the surface and inner zone in the

Table 1. FSW parameters of stir-in-plate for DP590 steel.

FSW parameter	Experimental condition (stir-in-plate)
Rotation direction	Clockwise
Tilting angle (˚)	2
Rotation speed (MPa)	600, 800, 1000
Traveling speed (mm/min)	120, 180, 240, 300, 360, 420

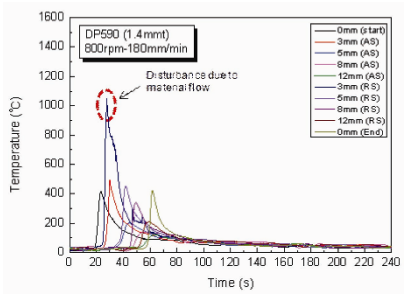

Fig. 3. Welding temperatures changes at the weld line during FSW.

FSW joints, followed by the vertical-direction crack in the surface area caused by cutting. Metallurgical inspection was also done on the cross-sections of the joints. They were polished and etched with a 5% Nital water solution (95 ml distilled water + 5 ml HNO_3) for the optical microscopic observations.

3. Results and discussion

3.1 Peak temperature of the FSW joint

FSW is a basically solid-state welding process for lower-melting-point materials such as aluminum alloys, but there is also an interest in using this process for AHSS. In spite of the recent research on the FSW of high-strength steels, the metal flow around the rotating tool and the temperature distributions in the workpiece are not yet completely understood. Above all, steel involves phase transformation depending on the thermal history during welding. This is an important fact that can be considered in determining the microstructure of the SZ and TMAZ near the tool probe. In addition, for the correct assessment of the welding deformation and the welding residual stress using thermal elastoplastic analysis, it is necessary to determine the temperature distribution in the workpiece as precisely as possible. Therefore, the peak temperature and its distribution should be directly obtained from the actual temperature measurement of the welding joint rather than from numerical simulation. Fig. 3 indicates the measured temperature directly under the probe and near the side when the rotation and traveling speeds were 800 rpm and 180 mm/min, respectively ($t = 0s$ is the temperature at the start of welding).

The temperature directly under the probe rapidly increased according to the measured point (time: 23.3 s; maximum temperature: 417°C). A sudden change in the temperature to 20°C was observed after the tool passed through the measuring

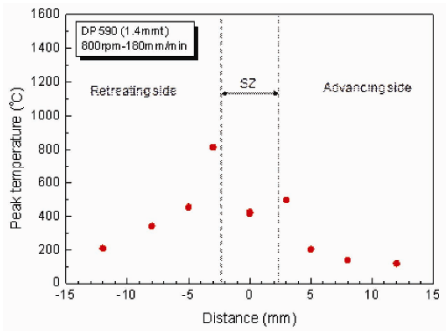

Fig. 4. Distribution of the peak temperatures at each point in the weld line.

point, and the time that it took to finish the welding was 79.9 s.

In the TMAZ, the temperature increased to around 900°C, and it was assumed that it reached the austenite temperature. The effect of the metal flow caused a disturbance in the measurement at the shoulder of the rotating tool. The cooling cycle was almost 24 s, and the average cooling speed was 29.2°C/s when the temperature decreased until 200°C from the peak temperature.

Fig. 4 shows that the peak temperature profiles at the advancing side (AS) and retreating side (RS) in the same point were asymmetrical, but that the temperature decreases near the base metal from the TMAZ and the HAZ were the same.

The temperature of the TMAZ influenced by the frictional heat between the tool shoulder and the probe was higher than that at the point directly under the probe. This result indicates that the heat input of the friction involving the shoulder is more predominant than that of the probe during FSW. Additionally, the temperature of the RS was higher than that of the AS because the direction of the metal flow was different. More specifically, shear motion generated in the direction opposite the tool rotating and traveling direction was observed in the AS point, as opposed to the extrusion effect generated in the same direction in the RS point. The extrusion effect is considered the reason of the high temperature at the RS point because it is possible to move the primary heated particle from the AS to the RS point.

The DP590 specimen after welding and after the measurement of the peak temperature is shown in Fig. 5. Based on this figure, it can be guessed that metal flow was generated near the SZ and TMAZ. For this reason, it can be said that there was temperature deviation. The measured temperature was under 1,000°C in the nearby SZ, which is lower than the 1,539°C melting point of steel. It was suggested that DP590 could be joined from the solid-state by the metal flow.

3.2 Effect of process parameters

The bead appearance of the FSW specimen with combined welding conditions is shown in Fig. 6. The useful boundaries of the welding conditions were a rotation speed of 120-420 mm/min and a traveling speed of 600-1000 rpm. A successful result was investigated among all the welding conditions. The

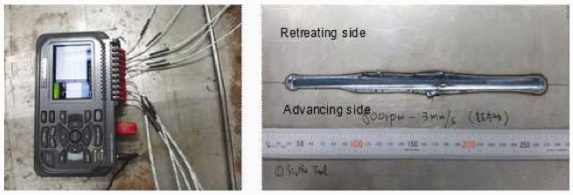

(a) Test recorder (b) Test specimen (800 rpm-180 mm/min)

Fig. 5. Test recorder view and specimen appearance of the welding temperature measurement during FSW.

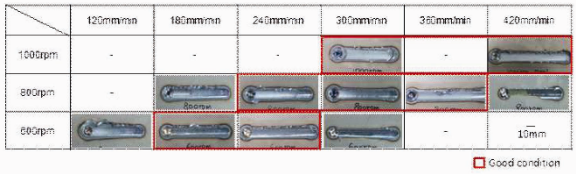

Fig. 6. Inspection of the FSW joints in various welding conditions through the bead appearance.

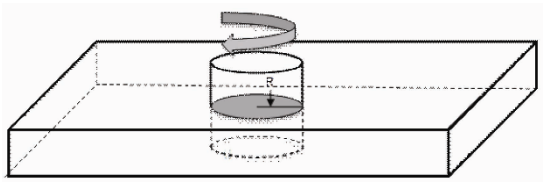

Fig. 7. Schematic diagram of the rotation of the shaft relative to the plate surface.

observed bead appearances of the welded specimens can be described as follows:

(1) Rough surface due to excessive burr.
(2) Welded joints included with surface defect.
(3) Sound bead without defect.

The heat input per unit length is related with the formation of welded joints and can be explained by Eq. (1) proposed by Frigaard [14]. The heat generation during FSW arises from two main sources: the friction at the surface of the tool and the deformation of the material around the tool.

When the cylindrical shaft relatively retained its mass rotation on the surface of the plate, the torque (M) could be explained as shown in Fig. 7.

$$M = \int_0^{M_R} dM = \int_0^R \mu P(r) 2\pi r^2 dr = 2/3 \mu \pi P R^3 \quad (1)$$

where M is the torque of the interface, μ is the friction coefficient, R is the radius of the tool shoulder, and $P(r)$ is the pressure per unit area. If the shearing energy is switched to frictional heat, the average heat input per unit area and the unit time will be as follows:

$$q = \int_0^{M_R} \omega dM = \int_0^R \omega 2\pi \mu P r^2 dr \quad (2)$$

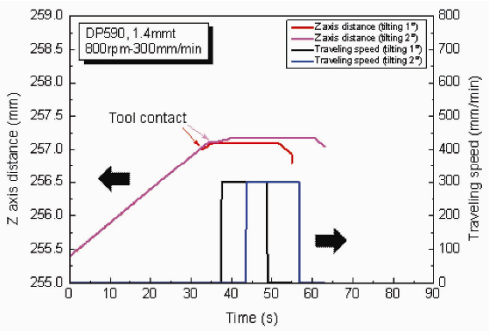

Fig. 8. Variations of the tool plunge depth at different tilting angles.

where q is the energy and ω is the angular velocity of the tool. To convert the angular velocity to the rotation speed, Eq. (3) was recalculated considering N (rotations/s), which is the rotation speed, and the transformation from ω to 2πN.

$$q=\int_0^R 4\pi^2\mu PNr^2dr=4/3\pi^2\mu PNR^3 . \quad (3)$$

Therefore, the heat input per unit length (Q) can indicate that the energy will be divided by the traveling speed during FSW (μ, P, and R are constant).

$$Q = q / V = (4/3)\pi^2\mu PNR^3 / V \propto N / V . \quad (4)$$

The heat input is expressed in a simple way by the rotation speed and traveling speed [15]. This equation indicates that the heat input is proportional to the rotation speed and inversely proportional to the traveling speed. Additionally, the contact area increment increases the amount of heat on the welded joints because the contact area is proportional to the plunge depth and is involved in the friction area. Observation was performed to evaluate the variance in plunge depth according to the changes in the angle and rotation speed.

Fig. 8 shows the variations in plunge depth at the 1 and 2° tilting angles. When the tilting angle was 1°, it was observed that the plunge depth decreased. It was seen that the decrease in the tilting angle led to an increase in the contact area between the shoulder and the base metal as well as to an increase in the heat input. The tilting angle should be carefully decided, however, because a decrease in the tilting angle is accompanied by an increase in the shearing stress on the welding tool. For this reason, 2° was accepted as securing the stability of the equipment for the experiment.

Figs. 9(a) and (b) show the variation in plunge depth under the rotation speed of 600 and 800 rpm, respectively. The plunge depth was unstable and shakiness occurred when the welding tool was rotated as a 600 rpm. On the other hand, it was observed that the plunge depth movement was stable and that the position was kept while rotating at a speed of 800 rpm.

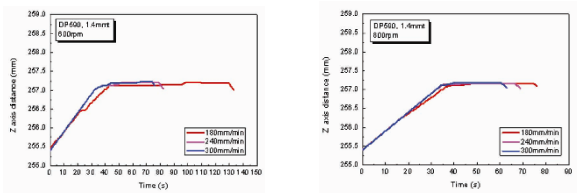

(a) Low rotation speed (600 rpm) (b) Optimum rotation speed (800 rpm)

Fig. 9. Relation between the tool plunge depth and the rotation speed at different traveling speeds.

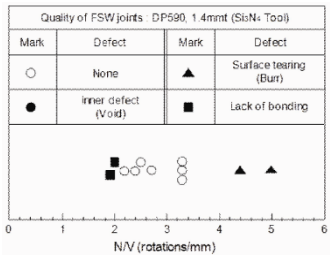

Fig. 10. Range of the optimum FSW conditions for DP590 steel.

3.3 Selection of the optimum welding condition

The range of the optimum FSW condition of DP590 is considered an important topic in terms of practical applications. The rotation speed, traveling speed, and tilting angle are the main independent factors largely influencing the joint quality. Actually, the three parameters are changing, and the others are fixed in the FSW experiment. The welding condition is usually determined depending on the target material, but it is known that the range of the optimum welding conditions was widened inversely proportional to the yield strength at a high temperature. According to the welding defect, an excessive burr on the bead was easily observed due to the large amount of heat input by the high rotation speed with a low traveling speed. Otherwise, when using a low rotation speed and a high traveling speed, the lack of heat input causes inner defects such as voids or groove-like linear defects on the joint surface. In severe cases, the probe is damaged.

Fig. 10 shows the boundary of the optimum welding condition without welding defect with respect to the main process parameters, which are the rotation and traveling speeds. The boundary of the optimum welding condition was extended with the increase in the rotation speed from 600 to 800 rpm. It seems that the metal flow activation was the major cause due to the improvement of the heat input, which was generated by the increase in rotation speed. It is possible to obtain the appropriate welded joints using a traveling speed of up to 420 mm/min at a rotation speed of 1000 rpm. In the case of excessive heat input made by a slow traveling speed when the rotation speed was constant, defects such as surface tearing, excessive burr, and wear of the tool probe were observed. On the contrary, insufficient heat input was indicated by the fast traveling speed. It was clearly observed that a groove-like defect along the weld line occurred due to the insufficient heat input.

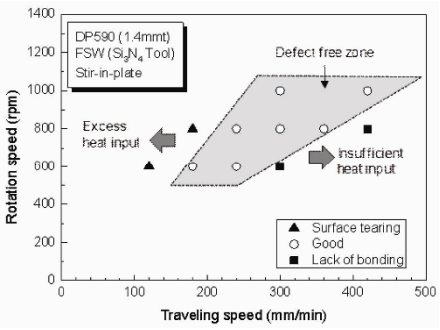

Fig. 11. Macrostructural feature of the surface defect joint (DP590, 1.4mmt).

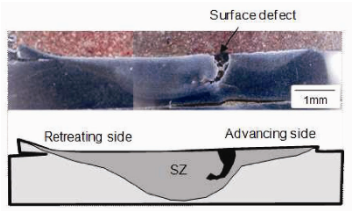

Fig. 12. Relation between the welding parameter, N/V and welded joint quality.

A surface defect occurred in the AS region, as shown in Fig. 11. This is because of the shearing motion, which was caused by the opposite directions of the metal flow around a rotating probe and a traveling workpiece.

3.4 Weld formation related with the N/V value

When the FSW process is performed, it is difficult to define the meaning of the heat input, but the definition from the number of rotations per unit length of the welded joint was conveniently used for calculating the heat input. Also, it is easy to understand the concept of physicality, and it is calculated as the ratio of the tool rotation speed and the traveling speed (N/V). Moreover, the reciprocal of this (V/N), called "revolution pitch," which is the amount of proceeds per tool rotation, has also been proposed.

Fig. 12 shows weldability separated by a symbol according to the heat input per unit length. As mentioned earlier, N/V means the relative ratio of the rotation speed to the traveling speed. The appropriate welded joints can be obtained using the N/V values within 2.2 to 4.2. In comparison, when the N/V values are smaller than 2.0, a surface defect appears. Burr or a rough surface is formed with N/V values of over 4.4. To confirm the inner defect in welded joints, X-ray radiography was conducted under each welding condition, such as 600, 800, and 1000 rpm rotation speeds, respectively, and a fixed traveling speed of 300 mm/min. In other words, the welding condition was used for three N/V values: 2.0, 2.7, and 3.3. Especially, no welding defect was observed not only in the three specimens but also in the specimen that used an N/V value of over 4.4.

4. Conclusions

In this study, the optimum welding condition and the effect of the friction stir welding (FSW) parameters on the quality of the welded joints of CR DP590 steel were investigated. The test results for the peak temperature distribution during FSW can be summarized as follows:

(1) It is possible to obtain the optimum welding condition using a Si_3N_4 tool made of ceramic material on stir-in-plate for DP 590 MPa-grade steel. The boundary of the optimum welding condition without welding defect was selected with several changes in the main parameters, such as the rotation speed of the tool and the traveling speed.

(2) The selected optimum welding parameter was used for the investigation of the peak temperature distribution near the rotating tool. As expected, the temperature in the TMAZ near the SZ increased to the austenite temperature of around 900°C, and temperature rapidly dropped immediately after welding.

(3) The N/V value, which was used to represent the heat input per unit length, showed a dominant effect on the joint quality. Appropriate welded joints were situated within the 2.2-4.2 N/V values. The insufficient heat input, however, generated a groove-like defect in the advancing side due to the low N/V values.

Acknowledgment

Financial support was provided by Korea Ministry of Planning and Budget Foundation through Korea Institute of Industrial Technology (KITECH).

Nomenclature

M	: Torque
μ	: Friction coefficient
R	: Radius of the tool shoulder
$P(r)$	: Pressure per unit area (P/A)
q	: Energy
ω	: Angular velocity
N	: Rotation speed (rpm)
Q	: Heat input per unit length
V	: Traveling speed (mm/min)

References

[1] W. M. Thomas, E. D. Nicholas, J. C. Needham, M. G. Murch, P. Templesmith and C. J. Dawes, *International Patent Application No.PCT/GB92/02203 and GB Patent Application No.9125978.8*, UK Patent Office, London (1991).

[2] C. G. Rhodes, M. W. Mahoney, W. H. Bingel, R. A. Spurling and C.C. Bampton, Effects of friction stir welding on microstructure of 7075 aluminum, *Scr. Mater.,* 36 (1997) 69-75.

[3] H. J. Liu, H. Fujii, M. Maeda and K. Nogi, Tensile properties and fracture locations of friction-stir-welded joints of 2017-T351 aluminum alloy, *J. Materials Processing Technology,* 142 (2003) 692-696.

[4] H. S. Choi, G. H. Park, W. S. Lim and B. M. Kim, Evaluation of weldability for resistance spot welded single-lap joint between GA 780DP and hot-stamped 22MnB5 steel sheets, *Journal of Mechanical Science and Technology,* 25 (6) (2001) 1543-1550.

[5] R. S. Mishra and Z. Y. Ma, Friction stir welding and processing, *Mater. Sci. and Eng., R* 50 (2005) 1-78.

[6] R. Nandan, T. Debroy and H. K. D. H. Bhadeshia, Recent advances in friction-stir welding – process, weldment structure and properties, *Prog. in Mater. Sci.,* 53 (2008), 980-1023.

[7] W. M. Thomas and E. D. Nicholas, Friction stir welding for the transportation industries, *Materials & Design,* 18 (1997) 269-273.

[8] F. Hayat, Comparing properties of adhesive bonding, resistance spot welding and adhesive weld bonding of coated and uncoated DP600 steel, *J. Iron and Steel Research, Inter.*, 18 (2011) 70-78.

[9] Y. G. Kim, H. Fujii, T. Tsumura, T. Komazaki and K. Nakata, Three defect types in friction stir welding of aluminum die casting alloy, *Mater. Sci. and Eng., A* 415 (2006) 250-254.

[10] K. S. Bang, K. J. Lee, H. S. Bang and H. S. Bang, Interfacial microstructure and mechanical properties of dissimilar friction stir welds between 6061-T6 aluminum and Ti-6%Al-4%V alloys, *Mater. Trans.,* 52 (2011) 974-978.

[11] K. J. Lee and S. H. Kim, Effects of tool plunge position on mechanical properties of friction-stir-welded region in A6061-T6/AZ31 dissimilar metals, *Journal of KWJS,* 30 (2012) 416-420.

[12] L. Yu, K. Nakata and J. Liao, Microstructural modification and mechanical property improvement in friction stir zone of thixo-molded AE42 Mg alloy, *J. Alloys and Compounds,* 480 (2009) 340-346.

[13] Y. S. Sato, M. Muraguchi and H. Kokawa, Tool wear and reactions in 304 stainless steel during friction stir welding, *Mater. Sci. Forum,* 675-677 (2011) 731-734.

[14] O. Frigaard, O. Grong and O. T. Midling: A process model for friction stir welding of age hardening aluminum alloys, *Metall. and Mater. Trans. A,* 32 (2001) 1189-1199.

[15] K. Nakata, Y. G. Kim, M. Ushio, T. Hashimoto and S. Jyogan, Weldability of high strength aluminum alloys by friction stir welding, *ISIJ Inter. Supple.*, 40 (2000) S15-S19.

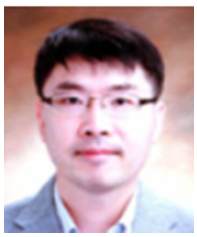

Young Gon Kim is a Senior Researcher in Department of Green Manufacturing Process R&D Group of KITECH. He received his M.S., Ph.D. degrees from Osaka University in Japan. His research interests include friction stir welding along with fusion welding process for automotive.

Ji Sun Kim is a Researcher in Department of Green Manufacturing Process R&D Group of KITECH. He received his B.S., M.S. degrees from Mokpo National University. His research interests are welding process analysis of fiber laser welding and spot welding.

In Ju Kim is a Principal Researcher in Department of Green Manufacturing Process R&D Group of KITECH. He received his M.S., Ph.D. degrees from Mokpo National University. His main research interests are automation of arc welding related with ship issues.